JOURNAL OF SOLID STATE CHEMISTRY 111, 300–309 (1994)

Temperature and Composition Dependence of the Cation Distribution in Synthetic $ZnFe_yAl_{2-y}O_4$ ($0 \leq y \leq 1$) Spinels

J. C. Waerenborgh,*,[1] M. O. Figueiredo,† J. M. P. Cabral,* and L. C. J. Pereira*

*Departamento de Química, ICEN, INETI, P2686 Sacavém Codex, Portugal; and †Centro Cristalografia e Mineralogia, IICT, Alam. D.Afonso Henriques 41-4°-E°, 1000 Lisboa, Portugal

Received August 9, 1993; accepted September 30, 1993

Members of the spinel solid solution series $ZnFe_yAl_{2-y}O_4$ (y = 0, 0.2, 0.4, 0.6, 1.0, 1.5, and 2) were synthesized by direct solid state reaction of the simple metal oxides in air at 1400 K. Two aliquots of the single-phase spinels obtained for each composition were annealed at 1350 and 1000 K for 48 hr and then quenched in water.

The structural study of the quenched samples was performed by powder XRD, using the Rietveld method of structure refinement. The inversion degrees estimated for $ZnFe_2O_4$ up to 1350 K are in good agreement with those published by O'Neill (*Eur. J. Mineral.* 4, 571 (1992)) in the range 773–1223 K. The nonlinear enthalpy of disordering model of O'Neill and Navrotsky (*Am. Mineral.* 68, 181 (1983); *Am. Mineral.* 69, 733 (1984)), recently applied to several studies of simple spinel oxides, could successfully describe the cation arrangement in spinels of the binary solid solution series prepared in this work, with parameters $\alpha_{Zn-Al} = +82$ kJ mole^{-1}, $\alpha_{Zn-Fe^3} = +46$ kJ mole^{-1}, $\beta = -20$ kJ mole^{-1}, and $\sigma = 0$.

^{57}Fe Mössbauer spectra collected at 300 and 80 K consisted of only one doublet. Although the contribution of tetrahedral Fe^{3+} could not be resolved, the variation of the estimated average hyperfine parameters with composition and quenching temperature could be correlated with the cation arrangement deduced from XRD data.

INTRODUCTION

Oxide spinels have long been a topic of interest in the solid state sciences because of their usefulness as magnetic materials, semiconductors, pigments, catalysts, and refractories. Being common accessory minerals, they are also of considerable interest in geochemistry as petrogenetic indicators and ores.

Spinels are a large class of compounds isotypic with the mineral spinel $MgAl_2O_4$. 2–3 oxide spinels have the general formula AB_2O_4, where A and B stand for divalent and trivalent cations, respectively. The ideal structural formula for a normal spinel is $A^tB_2^o\,[O_4]^c$, where t and o stand for tetrahedral and octahedral sites in a cubic close packing c of oxygens (4). The unit cell contains eight formula units and the symmetry is cubic, space group $Fd\bar{3}m$, number 227 (5). The anionic array is described by the monovariant equivalent position $32e''$, point symmetry $3m$; the actual values of the free parameter u (commonly known as the oxygen positional parameter) show a slight deviation from 1/4, the ideal value for cubic closest packing if the unit cell origin is taken at a center of symmetry $\bar{3}m$, equiposition 16c. This deviation usually takes the form of increasing the volume ratio between occupied tetrahedral and octahedral sites, respectively, 8a (1/8, 1/8, 1/8), $\bar{4}3m$, and 16d (1/2, 1/2, 1/2), $\bar{3}m$. A small fraction of additional interstitial positions, empty in an ideal stoichiometric spinel, may also be occupied, e.g., tetrahedral 8b and 48f or octahedral 16c (6).

For 2–3 spinels the inversion degree Λ is defined as the fraction of tetrahedral sites occupied by trivalent cations. Accordingly, for a normal spinel $\Lambda = 0$; for a completely inverted spinel $\Lambda = 1$ and the corresponding structural formula is $B^tA^oB^o\,[O_4]^c$.

Determination of the cation distribution is of considerable relevance to the solid state chemistry of spinels since theoretical interpretation of the chemical and physical properties of these compounds depends on the sites occupied by the cations. This knowledge is also of the utmost importance in the study of mineral equilibria.

Previous studies (7, 8) of natural Fe containing gahnite spinels, simplified formula $ZnAl_2O_4$, have drawn attention to the importance of the crystal chemistry of spinel solid solutions within the system ZnO–Al_2O_3–FeO–Fe_2O_3. Numerous contradictory results have been published for binary spinels of this system which may be explained by differences in sample preparation or thermal treatment as demonstrated by O'Neill (1), who established the cation distribution of $ZnFe_2O_4$ in the temperature range 773–1223

[1] To whom correspondence should be sent at present address: Institute for Transuranium Elements, CEC Joint Research Center, Postfach 2340, 76125 Karlsruhe, Germany.

0022-4596/94 $6.00

K. In the case of $ZnAl_2O_4$ the discrepancy of published results is much narrower (9–11) due to the very large tetrahedral and octahedral site preferences of Zn^{2+} and Al^{3+}, respectively (3 and references therein), which make the inversion degree of this oxide approximately zero even at high temperatures. Solid solutions of $ZnAl_2O_4$ and $ZnFe_2O_4$ have also been considered up to now essentially normal spinels (12–14).

In order to contribute to a better understanding of the crystal chemistry of spinels within the system $ZnO–Al_2O_3–FeO–Fe_2O_3$, structural investigations of the solid solution series $ZnFe_yAl_{2-y}O_4$ ($0 \leq y \leq 1$) and $Zn_{1-x}Fe_xAl_2O_4$ ($0 < x \leq 1$) were carried out (15). In this work we report the study of synthetic $ZnFe_yAl_{2-y}O_4$ spinels, equilibrated at two different temperatures. Both powder XRD, associated with the Rietveld method of structure refinement, and ^{57}Fe Mössbauer spectroscopy were used.

EXPERIMENTAL

Synthesis

In order to synthesize $ZnAl_{2-y}Fe_yO_4$ oxides (with y = 0.0, 0.1, 0.2, 0.6, 1.0, 1.5, and 2.0) the starting mixtures were prepared from α-Al_2O_3, ZnO, and α-Fe_2O_3 (Ventron, 99.99%) according to

$$(y/2)Fe_2O_3 + (1 - y/2)Al_2O_3 + ZnO \rightarrow ZnAl_{2-y}Fe_yO_4.$$

Adequate amounts of each starting oxide were ground together in a tungsten carbide mortar. The mixture was dry pressed into pellets (4 g each) which were sintered in air at 1450 K for several 48-hr periods. The grinding–dry pressing–sintering cycles were repeated for each sample until powder XRD and optical examination revealed only one homogeneous spinel phase. At the end of each cycle the weight of the pellets was controlled; it never varied more than 1 in 10^4, assuring that there was no significant loss of ZnO, which is consistent with previous results, particularly those of O'Neill (1), who found that this oxide is not perceptively volatile in air at temperatures below 1473 K. Two aliquots of each single-phase spinel were again dry pressed and heated in air for another 48 hr, one at 1000 K and the other at 1350 K. At the end of this period the pellets were dropped into water. Two sets of samples of the spinel solid solution series $ZnFe_yAl_{2-y}O_4$ ($0 \leq y \leq 1$), one equilibrated at T_{eq} = 1000 K and the other at T_{eq} = 1350 K, were thus obtained. 1350 K was chosen bearing in mind that the high-temperature cation distribution must be preserved during the quench. According to O'Neill and Navrotsky (3) it seems likely that below 1373 K the rates of cation redistribution in oxide spinels still allow effective quenching with normal techniques. Conversely, at low temperatures, enough time must be allowed for the cation distribution to achieve equilibrium. 1000 K was chosen because, according to O'Neill (1), for $ZnFe_2O_4$ above 700°C, an annealing time of 48 hr seems to be ample enough.

Pieces of a few pellets were examined by scanning electron microscopy with an energy dispersive system (SEM–EDS). Neither backscattered nor secondary electron images showed any heterogeneity on the specimen where the reaction was considered complete; conversely, $\simeq$1–10 μm grains rich in Al could be detected in samples from preliminary sintering experiments.

X-Ray Powder Diffraction Measurements and Structure Refinements

Finely ground sample powder (<10 μm) was back pressed into standard aluminium holders. Step scan powder diffraction intensities were collected with a Philips PW automated diffractometer system PW1710. A PW1820 Bragg Brentano goniometer fitted with a PW1752 curved graphite crystal monochromator, incident and diffracted beam Soller slits, 1° divergence and antiscatter slits, and a 0.2-mm receiving slit was used. The intensity measurements were made with a normal focus cobalt tube operated at 40 kV and 35 mA and using a take-off angle of 5°. The data were measured with a 2θ step size of 0.03° in a 2θ range of 15.00–143.00° and a counting time of 6 sec at each step.

Co was used instead of Cu radiation in the hope of improving the accuracy of the method. Fe and Zn have similar atomic numbers; however, as the wavelength of Co$K\alpha$ radiation is very close to the Fe absorption K edge, the difference between the scattering factors of Zn and Fe becomes larger for this radiation due to the anomalous scattering effect (cf., tables of dispersion corrections in 16–18).

The least-squares structure refinements were undertaken with the Rietveld powder profile program of Wiles and Young (19, 20) adapted to IBM-AT compatible microcomputers by Schneider (21).

The scattering factor for O^{2-} was obtained from (22) and those for Fe, Fe^{3+}, Zn, Zn^{2+}, Al, Al^{3+}, and O from (16). Anomalous dispersion coefficients were taken from (17, 18). Scattering factors for fully ionized species were used in final refinements because they always produced a slight improvement in the values of the agreement factors, R_B and R_{wp}, and negligible changes in the estimated values of the adjusted parameters.

An experimentally determined $K\alpha_1/K\alpha_2$ intensity ratio of 0.5 and a factor $\cos\theta_M = 0.735$ for the monochromator polarization correction (20) were used. This is the theoretically expected value for $\cos\theta_M$ in the case of Co$K\alpha$ radiation diffracted by the (002) plane of a graphite single crystal.

Two 2θ variable profile shape functions were used: Pseudo-Voigt

$$\wp\mathcal{L} + (1 - \wp)\mathcal{G}$$

with a fractional Lorentzian character $\wp = \wp_a + \wp_b\,(2\theta_i)$ and Pearson VII in which the exponent could vary according to

$$\mathbf{m} = \mathfrak{L}_a + \mathfrak{L}_b/(2\theta_i) + \mathfrak{L}_c/(2\theta_i)^2.$$

Pearson VII gave consistently the best R_B and R_{wp} values and was thus used in the final refinements. The peak full width at half maximum (FWHM) function of Caglioti *et al.* (23) was used. Background was also refined according to the function stated in Wiles and Young (20).

Rietveld refinements were conducted in three stages, assuming space group $Fd\bar{3}m$:

(i) Considering a normal cation distribution 20 parameters were fitted to the 4267 data points: one scale factor, six background parameters, zeropoint for 2θ, six profile function parameters (three for the mixing parameter **m** and three for the FWHM), one asymmetry correction, the cell parameter a_0, the oxygen positional parameter u, three isotropic thermal parameters (B), one for each equiposition 8*a*, 16*d*, and 32*e*.

(ii) The same as in (i) plus a cation disorder parameter K_F which allowed the occupation of the 8*a* and 16*d* sites by Zn^{2+} and Fe^{3+} to vary within the constraints of the ideal formula and full site occupancy; K_F was thus defined as the fraction of tetrahedral sites occupied by Fe^{3+} assuming all the Al^{3+} remained in the 16*d* position.

(iii) The same as in (ii) but this time the cation disorder parameter, K_A, was defined as the fraction of tetrahedral sites occupied by Al^{3+}, assuming all the Fe^{3+} remained in the 16*d* position.

Refinements were continued until the parameter shifts were less than 0.3 times the estimated standard deviations. Refinement of the preferred orientation parameter, as defined in (20), as well as of anisotropic temperature factors in 16*d* and 32*e* positions, had no effect on the final results. In stages (ii) and (iii), except for K_F and K_A, final estimated values for all the parameters as well as for the agreement factors were the same or, in the case of B parameters, did not differ by more than 1 standard deviation (Tables 1 and 2). Difference Fourier calculations (21) showed no residual electron density in interstitial positions 8*b*, 48*f* ($\simeq$3/8, 1/8, 1/8), or 16*c*.

Mössbauer Spectroscopy

Mössbauer spectra were performed in transmission mode using a conventional constant acceleration spectrometer and a 25-mCi ^{57}Co course in Rh matrix. The velocity scale was calibrated using an α-Fe foil at room temperature. Spectra were obtained at 300 and 80 K. Low-

TABLE 1

Final Results of the $ZnAl_{2-y}Fe_yO_4$ (T_{eq} = 1000 K) Powder XRD Structural Refinements (Stages (ii) and (iii)) Using the Rietveld Method[a]

y:	0.0	0.1	0.2	0.6	1.0	1.5	2.0
a_0	8.0883(2)	8.1051(3)	8.1238(2)	8.1922(4)	8.2662(5)	8.3554(3)	8.4432(3)
u	0.2642(1)	0.2642(1)	0.2642(1)	0.2631(1)	0.2626(2)	0.2614(2)	0.2603(1)
K_F	—	0.028(8)	0.024(6)	0.035(9)	0.066(8)	0.086(6)	0.100(5)
K_A	0.025(3)	0.013(4)	0.010(3)	0.015(4)	0.030(4)	0.038(3)	—
$B(8a)$	—	0.35(2)	0.44(2)	0.28(2)	0.40(3)	0.24(3)	0.50(2)
	0.36(2)	0.37(2)	0.45(2)	0.31(2)	0.36(3)	0.30(2)	—
$B(16d)$	—	0.39(4)	0.45(4)	0.50(4)	0.60(4)	0.57(3)	0.45(2)
	0.36(2)	0.37(4)	0.43(3)	0.47(4)	0.64(4)	0.51(3)	—
$B(32e)$	—	0.57(5)	0.76(5)	0.98(6)	1.24(5)	1.13(5)	0.79(4)
	0.54(4)	0.56(5)	0.75(5)	0.97(6)	1.24(5)	1.13(5)	—
R_{Bragg}	3.44	3.59	3.46	3.62	3.01	4.31	2.72
R_p	9.48	9.44	7.67	7.22	5.99	6.49	5.38
R_{wp}	12.30	12.37	10.77	9.29	7.89	8.35	7.05
$\mathcal{S}$	3.04	2.25	3.98	1.77	1.65	1.72	2.27

Note. K_F (K_A), fractions of tetrahedral sites occupied by Fe^{3+} (Al^{3+}) assuming all the Al^{3+} (Fe^{3+}) remain in the 16*d* position, were calculated in stages (ii) (iii). In both stages all the other parameters, except the B factors, refined to the same values.

[a] a_0, cell parameter (Å); u, oxygen positional parameter. The form of the isotropic temperature factors is $\exp\left[-2 \cdot B \cdot \left(\frac{\sin\theta}{\lambda}\right)^2\right]$ with B in Å^2.

R_{Bragg}, R_p, R_{wp}, and $\mathcal{S}$ agreement factors (as defined in Wiles and Young (19)). Numbers in parentheses denote one standard deviation of the least significant digit.

TABLE 2
Final Results of the $ZnAl_{2-y}Fe_yO_4$ (T_{eq} = 1350 K) Powder XRD Structural Refinements Using the Rietveld Method

y:	0.0	0.1	0.2	0.6	1.0	1.5	2.0
a_0	8.0888(2)	8.1047(3)	8.1231(2)	8.1952(3)	8.2682(3)	8.3571(3)	8.4409(3)
u	0.2639(1)	0.2641(1)	0.2639(1)	0.2624(1)	0.2620(1)	0.2608(1)	0.2590(1)
K_F	—	0.068(8)	0.074(6)	0.094(9)	0.134(8)	0.161(5)	0.201(6)
K_A	0.036(3)	0.030(4)	0.033(3)	0.041(4)	0.060(3)	0.071(5)	—
$B(8a)$	—	0.24(2)	0.31(2)	0.32(2)	0.28(2)	0.38(2)	0.41(2)
	0.32(2)	0.28(2)	0.35(2)	0.38(2)	0.37(2)	0.48(2)	—
$B(16d)$	—	0.32(4)	0.46(3)	0.47(3)	0.62(3)	0.55(3)	0.39(2)
	0.35(3)	0.27(3)	0.40(3)	0.41(3)	0.55(3)	0.47(3)	—
$B(32e)$	—	0.50(5)	0.75(5)	0.92(5)	1.10(5)	1.06(4)	0.83(4)
	0.56(4)	0.49(5)	0.73(5)	0.91(5)	1.10(5)	1.07(4)	—
R_{Bragg}	2.94	3.81	3.44	3.54	2.74	3.11	3.44
R_p	8.01	8.69	7.68	6.78	6.17	5.30	5.82
R_{wp}	10.20	11.62	10.42	8.88	7.91	7.02	7.56
$\mathcal{S}$	2.63	2.10	3.50	1.76	1.60	2.09	2.35

Note. Symbols are the same as in Table 1.

temperature measurements were performed using a liquid nitrogen flow cryostat. Absorbers were prepared by pressing the sample powder (≃5 mg of natural Fe/cm^2) into a perspex holder.

The spectra (Fig. 1) were fitted to Lorentzian peaks using a modified version (15) of the nonlinear least-squares computer method of Stone (24). No constraints were used during fitting. Estimated parameters are summarized in Table 3: isomer shifts, δ, given relative to metallic Fe at room temperature; quadrupole splittings, ΔE_Q; full widths at half maximum, Γ− and Γ+, of the low- and high-velocity peaks, respectively.

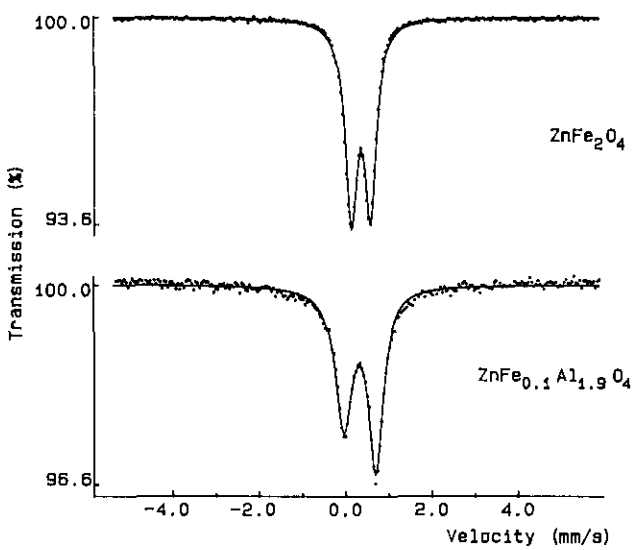

FIG. 1. Mössbauer spectra, taken at 300 K, of $ZnFe_2O_4$ and $ZnFe_{0.1}Al_{1.9}O_4$ equilibrated at 1350 K.

RESULTS AND DISCUSSION

Cation Distribution

Several additional refinements for each diffractogram assuming a cation distribution defined by $\Lambda = c\,K_F + (1 - c)\,K_A$ (with $0 \leq c \leq 1$) showed that the R factors, as well as the estimated values for the cell parameter and oxygen position, were always the same. The values of the isotropic temperature factors did not differ by more than 1 or 2 standard deviations. The analysis is, therefore,

TABLE 3
Mössbauer Parameters Estimated for the Doublet Fitted to the Spectra Collected at 300 K (Top) and 80 K (Bottom)

	T_{eq} = 1000 K				T_{eq} = 1350 K			
y	δ	ΔE_Q	Γ−	Γ+	δ	ΔE_Q	Γ−	Γ+
0.1	0.313	0.746	0.47	0.42	0.304	0.754	0.45	0.43
0.2	0.315	0.736	0.34	0.31	0.313	0.741	0.35	0.33
0.6	0.321	0.664	0.28	0.28	0.319	0.675	0.30	0.29
1.0	0.329	0.586	0.29	0.29	0.328	0.605	0.31	0.30
1.5	0.340	0.475	0.30	0.29	0.335	0.513	0.32	0.31
2.0	0.347	0.384	0.29	0.28	0.344	0.435	0.33	0.32
0.1	0.421	0.730	0.50	0.40	0.418	0.745	0.51	0.44
0.2	0.422	0.725	0.39	0.34	0.418	0.733	0.39	0.36
0.6	0.427	0.650	0.30	0.28	0.427	0.678	0.32	0.31
1.0	0.438	0.579	0.32	0.31	0.437	0.601	0.33	0.32
1.5	0.449	0.467	0.38	0.36	0.447	0.514	0.35	0.34
2.0	0.459	0.377	0.33	0.32	0.455	0.434	0.41	0.40

Note. δ, isomer shift given relative to metallic Fe at room temperature (mm/s); ΔE_Q, quadrupole splitting (mm/sec); Γ− Γ+, full widths at half maximum of the low- and high-velocity peaks, respectively (mm/s). Estimated standard deviations are ≤0.005 mm/sec.

not sensitive enough to distinguish if the inversion degree is due to Fe^{3+}, to Al^{3+}, or to both, which is not surprising since the average scattering factors (including the anomalous dispersion) for the 8*a* and 16*d* sites are the parameters which actually are optimized during the structure refinement and their values do not change significantly for $0 \leq c \leq 1$. This is also confirmed by the fact that the ratio K_F/K_A is 2.3 ± 0.1 for all diffractograms (Tables 1 and 2).

Results for the two sets of spinels of the solid solution series $ZnFe_yAl_{2-y}O_4$ ($0 \leq y \leq 1$), equilibrated at T_{eq} = 1000 K and T_{eq} = 1350 K, suggest that Λ increases with y and for the same y with T_{eq}; defining λ_F and λ_A as the fraction of tetrahedral sites occupied by Fe^{3+} and Al^{3+} respectively, the whole range of results corresponding to $\Lambda = \lambda_F + \lambda_A = c\,K_F + (1 - c)\,K_A$ with $0 \leq c \leq 1$, is, however, consistent with experimental data.

An attempt was made to estimate the value of c corresponding to a solution which minimized the difference between the radii calculated from the interatomic distances and the average cation radii.

The interatomic distances between a cation and the nearest anion are given by (25)

$$d_t = a_0\sqrt{3}(u - 0.125) \quad \text{for the } 8a \text{ site} \qquad [1]$$

$$d_o = a_0(3u^2 - 2u + 0.375)^{1/2} \quad \text{for the } 16d \text{ site.} \qquad [2]$$

From these values cation radii (hereafter referred to as structural radii) may be estimated taking

$$r_t = d_t - r_{O^{2-}} \quad \text{and} \quad r_o = d_o - r_{O^{2-}} \qquad [3]$$

assuming that the radius of tetrahedrally coordinated O^{2-} is $r_{O^{2-}} \simeq 1.38$ Å (26).

Four sets of average cation radii, $\langle r\rangle_t$ and $\langle r\rangle_o$ for the 8*a* and the 16*d* sites, respectively, were calculated for each spinel (Table 4). The first two sets correspond to the cation distribution defined by $\Lambda = \lambda_A = K_A$ ($c = 0$) and were calculated according to

$$\langle r\rangle_t = (1 - K_A)(r_{Zn^{2+}})_t + (K_A)(r_{Al^{3+}})_t \qquad [4]$$

$$\langle r\rangle_o = ((2 - y - K_A)(r_{Al^{3+}})_0 + (y)(r_{Fe^{3+}})_o + K_A(r_{Zn^{2+}})_o)/2 \qquad [5]$$

using in set 1 the effective cation radii (r_X) of Shannon (26), Sh radii, and in set 2 those of O'Neill and Navrotsky (2), NN radii. The third and fourth sets correspond to the cation distribution defined by $\Lambda = \lambda_F = K_F$ ($c = 1$),

$$\langle r\rangle_t = (1 - K_F)(r_{Zn^{2+}})_t + (K_F)(r_{Fe^{3+}})_t \qquad [6]$$

$$\langle r\rangle_o = ((2 - y)(r_{Al^{3+}})_o + (y - K_F)(r_{Fe^{3+}})_o + K_F(r_{Zn^{2+}})_o)/2 \qquad [7]$$

using in the third set the effective cation radii (r_X) of Shannon (26) and in the fourth set those of O'Neill and Navrotsky (2).

TABLE 4
Cation Radii in 8*a* (t) and 16*d* (o) Sites in Spinels

y	T_{eq} = 1000 K				T_{eq} = 1350 K			
0.0	0.57				0.57			
	0.53				0.53			
	0.59	0.58	—	—	0.59	0.57	—	—
	0.54	0.53	—	—	0.54	0.53	—	—
0.1	0.57				0.57			
	0.54				0.54			
	0.60	0.58	0.60	0.58	0.59	0.57	0.59	0.57
	0.54	0.54	0.54	0.54	0.54	0.54	0.54	0.54
0.2	0.58				0.57			
	0.54				0.55			
	0.60	0.58	0.60	0.58	0.59	0.57	0.59	0.57
	0.55	0.54	0.55	0.54	0.55	0.55	0.55	0.57
0.6	0.58				0.57			
	0.57				0.57			
	0.60	0.58	0.60	0.58	0.59	0.57	0.59	0.57
	0.57	0.57	0.57	0.57	0.57	0.57	0.57	0.57
1.0	0.59				0.58			
	0.59				0.59			
	0.59	0.57	0.59	0.57	0.59	0.57	0.59	0.57
	0.59	0.59	0.59	0.59	0.60	0.59	0.60	0.59
1.5	0.59				0.59			
	0.62				0.62			
	0.59	0.57	0.59	0.57	0.59	0.57	0.58	0.56
	0.62	0.62	0.62	0.62	0.62	0.62	0.63	0.62
2.0	0.60				0.58			
	0.65				0.66			
	—	—	0.59	0.57	—	—	0.58	0.56
	—	—	0.65	0.65	—	—	0.66	0.65

Note. Estimated standard deviations are ≤0.01 Å. Values in each partition of the table represent:

radii calculated from u and a_0, Eqs. [1]–[3]: r_t / r_o

average cation radii Eqs. [4]–[7]:	set 1	set 2	set 3	set 4
	$\langle r_{Sh}\rangle_t$	$\langle r_{NN}\rangle_t$	$\langle r_{Sh}\rangle_t$	$\langle r_{NN}\rangle_t$
	$\langle r_{Sh}\rangle_o$	$\langle r_{NN}\rangle_o$	$\langle r_{Sh}\rangle_o$	$\langle r_{NN}\rangle_o$
	(taking $\Lambda = K_A$)		(taking $\Lambda = K_F$)	

K_F is larger than K_A and, for each coordination, $r_{Zn^{2+}} - r_{Al^{3+}} > r_{Zn^{2+}} - r_{Fe^{3+}}$. These two effects compensate each other, and both $\langle r\rangle_t$ and $\langle r\rangle_o$ are the same within experimental error for all cation distributions defined by $0 \leq c \leq 1$. For the $ZnFe_yAl_{2-y}O_4$ spinels, as far as the cation distribution is concerned, this treatment is therefore inconclusive.

An interesting variation of the $(Zn^{2+})^t$–O^{2-} interatomic distance along the series is however inferred from Table 4.

Sets 2 and 4 of average cation radii should be closer to the structural radii because the NN effective cation radii were optimized for oxide spinels. While this is indeed observed for $y \leq 0.6$, for $y \geq 1.0$ and in the case of the tetrahedral radii the agreement is much better with sets 1 and 3. Differences between NN and Sh radii of Al^{3+}, Fe^{3+}, and Zn^{2+} are only significant in the case of tetrahedrally coordinated Zn^{2+} (0.58 and 0.60 Å, respectively). The above trend seems thus to indicate an increase of the interatomic distance $(Zn^{2+})^t$–O^{2-} with y. Further comments on this matter will be suggested by Mössbauer results.

Thermodynamic Modeling

A quantitative model of the change in the degree of inversion Λ of binary spinels with quench temperature T_{eq} was proposed by O'Neill and Navrotsky (2). From lattice energy arguments they concluded that the enthalpy of mixing of different cations A and B on equivalent crystallographic sites, ΔH_D, varies with Λ according to $\alpha_{A-B}\,\Lambda + \beta_{A-B}\,\Lambda^2$.

The equilibrium cation distribution may be obtained when the free energy of disordering

$$\Delta G_D = \Delta H_D - T_{eq}\,(\Delta S_C + \Delta S_D)$$

for the interchange reaction

$$(A^{2+})^t + (B^{3+})^o \rightarrow (A^{2+})^o + (B^{3+})^t$$

is at a minimum with respect to Λ, i.e., $(\partial \Delta G_D/\partial \Lambda)_T = 0$. Considering that the change in configurational entropy is given by

$$\Delta S_C = -R[\Lambda \ln \Lambda + (1-\Lambda)\ln(1-\Lambda) + \Lambda \ln(\Lambda/2) + (2-\Lambda)\ln(1-\Lambda/2)]$$

(ΔS_D is the nonconfigurational entropy of disordering) the following relationship is derived:

$$-RT_{eq}\ln\left[\frac{\Lambda^2}{(1-\Lambda)(2-\Lambda)}\right] = \alpha_{A-B} + 2\beta_{A-B}\Lambda - T_{eq}\Delta S_D. \quad [8]$$

The α_{A-B} term may be split according to $\alpha_{A-B} = \alpha_A - \alpha_B$ into structurally invariant site preference energies α_A and α_B characteristic of the A and B species. The available empirical evidence (1, 3, 27–29) shows that the β_{A-B} term may be treated as a constant $\simeq -20$ kJ mole^{-1} for 2–3 spinels. As far as the excess entropy of mixing, ΔS_D, is concerned, O'Neill and Navrotsky (2) suggested that the main contribution to its value comes from the crystal field electronic effect and may be expressed as $\sigma_{A-B}\,\Lambda$. In the cases of Fe^{3+}, Al^{3+}, and Zn^{2+} it is expected to be zero.

Considering Λ estimated from the Rietveld data of $ZnAl_2O_4$ and $ZnFe_2O_4$ equilibrated at 1350 K, $\beta = -20$ kJ mole^{-1} and $\sigma = 0$ one obtains

$$\alpha_{Zn-Al} = \alpha_{Zn} - \alpha_{Al} = +82 \text{ kJ mole}^{-1};$$

$$\alpha_{Zn-Fe^3} = \alpha_{Zn} - \alpha_{Fe^3} = +46 \text{ kJ mole}^{-1}.$$

These values are in reasonably good agreement with those estimated by O'Neill and Navrotsky (3), $\alpha_{Zn-Al} \simeq 89$ kJ mole^{-1} and $\alpha_{Zn-Fe^3} \simeq 53$ kJ mole^{-1}, considering the scarcity and inconsistency of data then available. More relevant is the similarity between the values of α_{Zn-Fe^3} found in this work and estimated by O'Neill (1) for $ZnFe_2O_4$ equilibrated in the temperature range 773–1223 K, when β was constrained to be equal to -20 kJ mole^{-1}. Values published in (1) for spinels equilibrated above 1223 K are, according to the author, inconsistent with the other results because they were not perfectly quenched.

The extension of this thermodynamic approach to the binary spinel solid solutions is straightforward (3). Cation distribution in the $ZnFe_yAl_{2-y}O_4$ spinels may be described by

	Zn^{2+}	Fe^{3+}	Al^{3+}
8*a*	$1 - \lambda_F - \lambda_A$	λ_F	λ_A
16*d*	$\lambda_F + \lambda_A$	$y - \lambda_F$	$2 - y - \lambda_A$

Equilibrium cation distribution may be obtained when the free energy

$$\Delta G_D = \Delta H_D - T_{eq}(\Delta S_C + \Delta S_D)$$

for the interchange reaction

$$\Lambda(Zn^{2+})^t + \lambda_A(Al^{3+})^o + \lambda_F(Fe^{3+})^o \rightarrow \Lambda(Zn^{2+})^o + \lambda_A(Al^{3+})^t + \lambda_F(Fe^{3+})^t$$

with $\Lambda = \lambda_F + \lambda_A$ is at a minimum with respect to any change in the disorder parameters λ_F and λ_A. For these solid solutions

$$\Delta H_D = [\alpha_{Zn-Fe^3} + \beta(\lambda_F + \lambda_A)]\lambda_F + [\alpha_{Zn-Al} + \beta(\lambda_A + \lambda_F)]\lambda_A$$

$$\Delta S_D = \sigma_{Zn-Fe^3}\lambda_F + \sigma_{Zn-Al}\lambda_A$$

$$\Delta S_C = (1-\lambda_F-\lambda_A)\ln(1-\lambda_F-\lambda_A) + \lambda_F \ln(\lambda_F) + \lambda_A \ln(\lambda_A) + \frac{\lambda_F+\lambda_A}{2}\ln\left(\frac{\lambda_F+\lambda_A}{2}\right) + \frac{y-\lambda_F}{2}\ln\left(\frac{y-\lambda_F}{2}\right) + \frac{2-y-\lambda_A}{2}\ln\left(\frac{2-y-\lambda_A}{2}\right).$$

Differentiating ΔG_D with respect to λ_A and λ_F

$$\frac{\partial \Delta G_D}{\partial \lambda_A} = \alpha_{Zn-Al} + 2\beta(\lambda_F + \lambda_A) - T_{eq}\left(\frac{\partial \Delta S_C}{\partial \lambda_A} + \sigma_{Zn-Al}\right)$$

$$\frac{\partial \Delta G_D}{\partial \lambda_F} = \alpha_{Zn-Fe^3} + 2\beta(\lambda_F + \lambda_A) - T_{eq}\left(\frac{\partial \Delta S_C}{\partial \lambda_F} + \sigma_{Zn-Fe^3}\right)$$

with

$$\frac{\partial \Delta S_C}{\partial \lambda_A} = \frac{\lambda_A(\lambda_F + \lambda_A)}{(1 - \lambda_F - \lambda_A)(2 - y - \lambda_A)} \quad \text{and}$$

$$\frac{\partial \Delta S_C}{\partial \lambda_F} = \frac{\lambda_F(\lambda_F + \lambda_A)}{(1 - \lambda_F - \lambda_A)(y - \lambda_F)}.$$

Making $\partial \Delta G_D/\partial \lambda_F = 0$ and $\partial \Delta G_D/\partial \lambda_A = 0$ to find the minimum of ΔG_D,

$$-RT_{eq} \ln\left[\frac{\lambda_A(\lambda_F + \lambda_A)}{(1 - \lambda_F - \lambda_A)(2 - y - \lambda_A)}\right] = \alpha_{Zn-Al} + 2\beta(\lambda_F + \lambda_A) - T_{eq}\sigma_{Zn-Al} \quad [9]$$

$$-RT_{eq} \ln\left[\frac{\lambda_F(\lambda_F + \lambda_A)}{(1 - \lambda_F - \lambda_A)(y - \lambda_F)}\right] = \alpha_{Zn-Fe^3} + 2\beta(\lambda_F + \lambda_A) - T_{eq}\sigma_{Zn-Fe^3}. \quad [10]$$

From these two equations it is possible to estimate numerically λ_A and λ_F for each composition y and for each equilibrium temperature, 1000 and 1350 K (Table 5).

Values of $\Lambda = \lambda_A + \lambda_F$ theoretically calculated are plotted as curves on a graph of Λ vs y (Fig. 2). Approximate experimental values $\Lambda_{exp} = \lambda_{Aexp} + \lambda_{Fexp}$, with $\lambda_{Aexp} = (1 - c)\ K_A$ and $\lambda_{Fexp} = c\ K_F$ (Table 6), are also plotted in the same figure. c values were estimated assuming that the ratio $\lambda_{Aexp}/\lambda_{Fexp}$ was equal to the theoretically predicted ratio λ_A/λ_F. Except for $ZnAl_2O_4$, T_{eq} = 1000 K, the difference between the theoretical and experimental values of the inversion degrees, $\Lambda - \Lambda_{exp}$, is less than 1.5 times the estimated standard deviations of the experimental Λ values. Since $ZnAl_2O_4$, T_{eq} = 1000 K, has the lowest inversion degree, the accuracy of the value estimated from XRD data is probably the poorest, thus explaining the largest difference relative to the theoretical calculations.

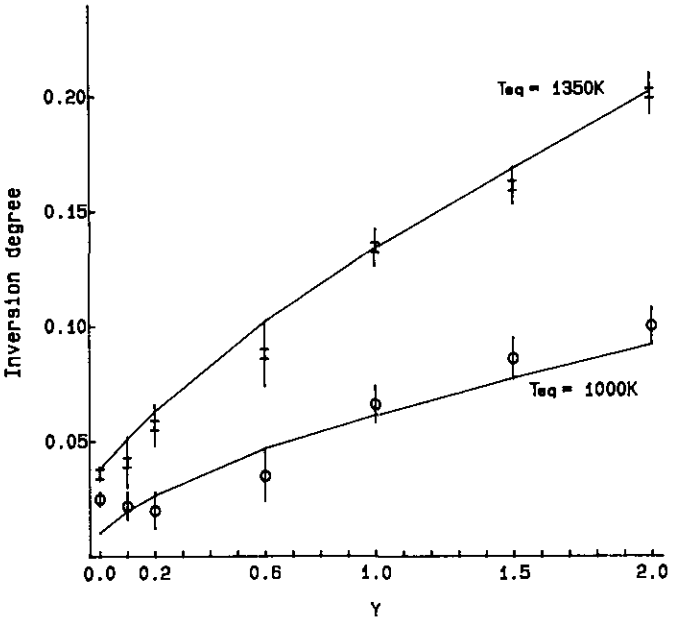

FIG. 2. Inversion degrees, $\Lambda = \lambda_F + \lambda_A$, calculated according to Eqs. [8]–[10] (solid lines) and estimated from powder XRD structural refinements, (I, T_{eq} = 1350 K; O, T_{eq} = 1000 K).

TABLE 5

Fraction of Tetrahedral Sites Occupied by Fe^{3+} and Al^{3+}, λ_F and λ_A, Calculated by the Thermodynamic Model of O'Neill and Navrotsky (2, 3) Assuming $\alpha_{Zn-Al} = 82$ kJ/mole, $\alpha_{Zn-Fe^3} = 46$ kJ/mole, $\beta = -20$ kJ/mole, and no Excess Entropy of Disordering

	T_{eq} = 1000 K		T_{eq} = 1350 K	
y	λ_F	λ	λ_F	λ_A
0	—	0.010	—	0.038
0.1	0.015	0.005	0.024	0.028
0.2	0.023	0.004	0.041	0.022
0.6	0.044	0.002	0.090	0.012
1.0	0.060	0.001	0.127	0.007
1.5	0.077	0.0004	0.166	0.003
2.0	0.092	—	0.202	—

Cell Edges and Oxygen Positional Parameters

Larger a_0 cell edges are associated with increasing substitution of Fe^{3+} for Al^{3+} as a direct consequence of the larger cation radius of the former cation. Due to the large

TABLE 6

Fraction of Tetrahedral Sites Occupied by Fe^{3+} and Al^{3+}, $\lambda_{F_{exp}}$ and $\lambda_{A_{exp}}$, Respectively, Based on XRD Data and Assuming $\lambda_{A_{exp}}/\lambda_{F_{exp}} = \lambda_A/\lambda_F$ (cf. Table 5)

	T_{eq} = 1000 K		T_{eq} = 1350 K	
y	$\lambda_{F_{exp}}$	$\lambda_{A_{exp}}$	$\lambda_{F_{exp}}$	$\lambda_{A_{exp}}$
0.1	0.016(8)	0.005(1)	0.019(2)	0.022(4)
0.2	0.017(6)	0.003(1)	0.039(2)	0.018(2)
0.6	0.032(9)	0.0014(4)	0.075(9)	0.009(1)
1.0	0.064(8)	0.0011(2)	0.119(8)	0.0066(3)
1.5	0.085(6)	0.0004(1)	0.155(5)	0.0028(2)

correlation between the zero point for 2θ and a_0, common in similar refinements (27), the accuracy of the estimated values for this parameter is, probably, considerably worse than that implied by the estimated standard deviations. Therefore, present data do not warrant a more detailed analysis of the a_0 variation with y and T_{eq}.

The oxygen positional parameter (u) variation with y and T_{eq} (Fig. 3) may be explained considering that u decreases with the ratio r_t/r_o (cf. Eqs. [1] and [2]). As $ZnFe_yAl_{2-y}O_4$ ($0 \leq y \leq 1$) spinels are largely normal (i.e., $\Lambda < 0.33$) and the Fe^{3+} cation radius is larger than the Al^{3+} one, the composition dependence of u observed in Fig. 3 is not surprising. On the other hand, for each spinel, u is lower for the higher equilibration temperature and the difference between the estimated values of u for T_{eq} = 1350 K and T_{eq} = 1000 K increases with y. This is consistent with the experimental values of the inversion degree, considering that increasing Λ corresponds to increasing the number of small trivalent cations occupying the tetrahedral sites and larger divalent cations the octahedral sites.

Mössbauer Spectra

Mössbauer spectra of all the samples are consistent with those obtained by Rüegsegger *et al.* (12), Prakash (13), and O'Neill (1), showing only two peaks which could be fitted with one doublet with parameters typical of ferric iron (Fig. 1 and Table 3). The quadrupole splittings measured at 300 and 80 K for each sample are the same within experimental error; the increase in the isomer shifts as temperature decreases is explained by the second-order Doppler shift.

For $ZnFe_yAl_{2-y}O_4$ samples with $y \geq 0.6$ the estimated widths and relative areas for both peaks in each spectrum were equal within experimental error. In the spectra of $ZnFe_{0.1}Al_{1.9}O_4$ and $ZnFe_{0.2}Al_{1.8}O_4$ the low-velocity peak is broader, and this broadening is more pronounced in the spectra taken at 80 K and for the samples with lower iron content. The asymmetry of the doublet in these spectra may be explained by the slow spin–spin relaxation of the Fe^{3+} spins due to the low concentration of this cation in a diamagnetic matrix (12). As the electronic ground state of Fe^{3+} in these oxides is ^6S, which is characterized by a vanishing orbital momentum, spin–lattice interaction may be considered negligible (30). The low-velocity peak in the Mössbauer spectra of the $ZnFe_{0.1}Al_{1.9}O_4$ and $ZnFe_{0.2}Al_{1.8}O_4$ samples is broader than the high-velocity peak, and thus corresponds to the $\pm 1/2 \rightarrow \pm 3/2$ nuclear transition of ^{57}Fe, showing that the main component of the electric field gradient, V_{zz}^{lat}, in the 16*d* site of these spinels is negative (12). There is experimental evidence that this parameter is also negative in $ZnAl_2O_4$ (^{27}Al nuclear magnetic resonance data from Brun (31)) and $ZnFe_2O_4$ (Mössbauer measurements in an external magnetic field by Evans *et al.* (32)).

The variations of δ and ΔE_Q with composition, y, for both temperatures 1000 and 1350 K (Fig. 4) are similar to those observed by Rüegsegger *et al.* (12). The increase in δ with Fe content may be correlated with the increase

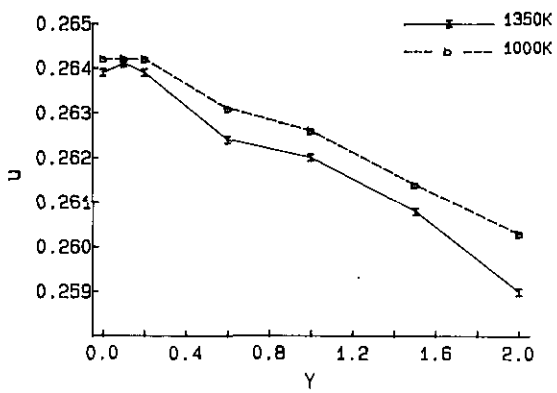

FIG. 3. Oxygen positional parameters, u, estimated from powder XRD structural refinements of $ZnFe_yAl_{2-y}O_4$ spinels, equilibrated at 1350 and 1000 K. The connecting lines are guides to the eye.

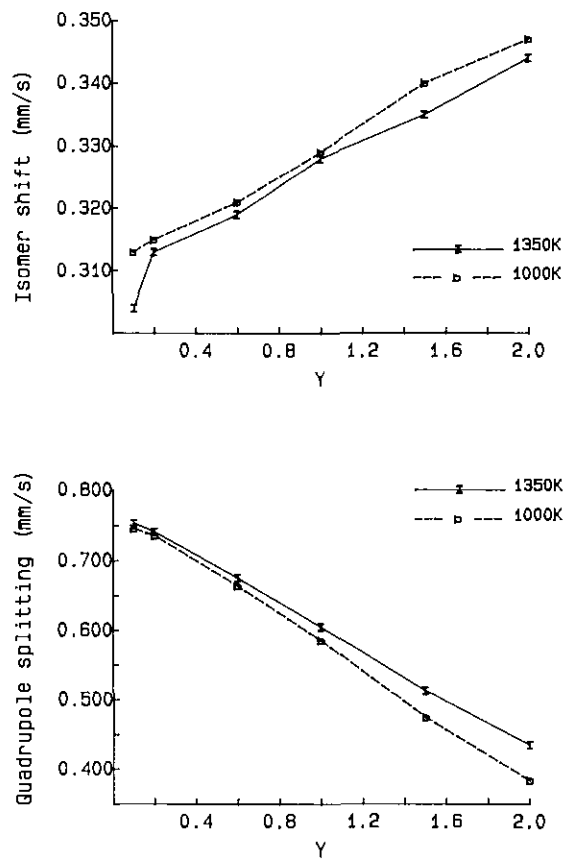

FIG. 4. Isomer shifts, δ, and quadrupole splittings, ΔE_Q, estimated from the Mössbauer spectra taken at 300 K of $ZnFe_yAl_{2-y}O_4$ spinels equilibrated at 1350 and 1000 K. The connecting lines are guides to the eye.

in both r_t and r_o (Table 4) as well as with the inductive effect, as defined by Menil (33), of the competing bonds $D-O^{2-}$ involving the O^{2-} anions which are chemically bonded to both a cation D and Fe^{3+}; in the spinel structure, the ionicity of a certain $Fe^{3+}-O^{2-}$ bond is expected to be larger the more electronegative the other three cations coordinating the same O^{2-} are. The average number of Fe^{3+} cations relative to the average number of Al^{3+} cations bonded to a O^{2-} increases with y and, since Fe^{3+} is more electronegative than Al^{3+} (34), the ionicity of the $Fe^{3+}-O^{2-}$ bonds and therefore the δ of the Fe^{3+} are expected to increase with y. A similar increase in ionic character of the $Zn^{2+}-O^{2-}$ bond might be related with the already mentioned increase in the $(Zn^{2+})^t-O^{2-}$ interatomic distance along the solid solution series.

The decrease in ΔE_Q with increasing y can be explained assuming that the contribution to the spectra of Fe^{3+} in 16*d* positions, $(Fe^{3+})^o$, dominates, in good agreement with XRD data. According to theoretical calculations (35) V_{zz}^{lat} in the 16*d* sites in spinels decreases as u increases; as mentioned above there is experimental evidence that it is negative for both end members of the solid solution series $ZnFe_yAl_{2-y}O_4$. Considering the variation of u with y (Fig. 3) ΔE_Q of octahedral Fe^{3+} is thus expected to decrease with increasing iron content (the similarities of Fig. 3 and the plot of ΔE_Q vs y in Fig. 4 are remarkable).

For all compositions, spinels equilibrated at 1000 K have a higher δ and a lower ΔE_Q than those equilibrated at 1350 K. Both features may be related to a nonzero inversion degree. Since δ usually decreases with coordination number (33), the larger the contribution of tetrahedrally coordinated Fe^{3+}, $(Fe^{3+})^t$, to a certain spectrum, the lower the δ estimated for that spectrum envelope should be. On the other hand, u variation with quenching temperature would point to a variation of ΔE_Q opposite to the observed one. ΔE_Q variation must then be related to other factors, probably to the different relative areas of the $(Fe^{3+})^o$ and $(Fe^{3+})^t$ contributions to the Mössbauer spectra. $(Fe^{3+})^t$, although in a position with cubic symmetry, is expected to have a nonzero ΔE_Q due to the noncubic symmetry of the electric charge distribution in the vicinity of the 8*a* position, created by the occupation of the same equipoints by chemically different cations (36, 37). The relative magnitudes of $(Fe^{3+})^o$ and $(Fe^{3+})^t$ quadrupole splittings are, however, difficult to estimate.

CONCLUSION

The thermodynamic treatment of O'Neill and Navrotsky (2, 3) was already used in the study of simple spinel oxides; e.g., $NiAl_2O_4$ (27, 29), $ZnFe_2O_4$ (1), and $MgFe_2O_4$ (28). In this work it could also successfully model the temperature and composition variation of the cation distribution in spinels of the binary solid solution series $ZnFe_yAl_{2-y}O_4$.

Due to the difficulty in estimating from XRD data the distribution of three different cations in two different equipoints and the inability of ^{57}Fe Mössbauer spectroscopy to resolve tetrahedral and octahedral Fe^{3+} contributions to the spectra of these spinels, cation arrangements in the ternary spinels could not be unambiguously determined from experimental data alone. Considering the thermodynamic parameters calculated from the results obtained for $ZnAl_2O_4$ and $ZnFe_2O_4$ equilibrated at T_{eq} = 1350 K ($\alpha_{Zn-Al} = +82$ kJ mole^{-1}, $\alpha_{Zn-Fe^3} = +46$ kJ mole^{-1} assuming $\beta = -20$ kJ mole^{-1} and $\sigma = 0$), theoretical values for the number of Fe^{3+} and Al^{3+} cations in 8*a* positions, λ_A and λ_F, were calculated for all the samples (Table 5). Values based on XRD data, λ_{Aexp} and λ_{Fexp}, could then be estimated (Table 6), assuming $\lambda_{Aexp}/\lambda_{Fexp} = \lambda_A/\lambda_F$. Calculated and experimental inversion degrees, except for the spinel with the lowest inversion degree, differ by less than 1.5 times the standard deviations estimated for the experimental values (Fig. 2). In good agreement with the relative site preference energies of Al^{3+} and Fe^{3+} ((3) and references therein) the fraction of Fe^{3+} in tetrahedral coordination is always larger than the corresponding fraction of Al^{3+}.

As far as $ZnFe_2O_4$ is concerned, the Λ values of this spinel quenched from 1000 and 1350 K (as well as the estimated $\alpha_{Zn-Fe^3} = +46$ kJ mole^{-1}) are in excellent agreement with the results of O'Neill (1) obtained for several $ZnFe_2O_4$ samples quenched from different temperatures in the range 773–1273 K. It seems, therefore, that it is not impossible to quench the equilibrium cation distribution in $ZnFe_2O_4$ at least up to 1350 K.

ACKNOWLEDGMENTS

The authors are indebted to Dr. A. Correia dos Santos and the Chemistry Department of the Faculty of Sciences of the University of Lisbon for the use of the X-ray powder diffractometer.

REFERENCES

1. H. St. C. O'Neill, *Eur. J. Mineral.* **4,** 571 (1992).
2. H. St. C. O'Neill and A. Navrotsky, *Am. Mineral.* **68,** 181 (1983).
3. H. St. C. O'Neill and A. Navrotsky, *Am. Mineral.* **69,** 733 (1984).
4. J. Lima-de-Faria and M. O. Figueiredo, *J. Solid State Chem.* **16,** 7 (1976).
5. "International Tables for Crystallography—Vol. A: Space-Group Symmetry" (T. Hahn, Ed.). Reidel, Dordrecht, The Netherlands, 1983.
6. A. Preisinger, *Fortsch. Mineral.* **61,** 153 (1983).
7. M. O. Figueiredo, A. Penna-Costa, and J. C. Waerenborgh, *Garcia de Orta, Ser. Geol.* **10,** 27 (1987).
8. J. C. Waerenborgh, H. Annersten, T. Ericsson, M. O. Figueiredo, and J. M. P. Cabral, *Eur. J. Mineral.* **2,** 267 (1990).

9. P. Fischer, *Z. Kristallogr.* **124,** 275 (1967).
10. R. F. Cooley and J. S. Reed, *J. Am. Ceram. Soc.* **55,** 395 (1972).
11. C. O. Arean, J. S. D. Vinuela, J. M. R. Gonsalez, and A. M. Arjona, *Mater. Chem.* **6,** 165 (1981).
12. P. Rüegsegger, F. Waldner, and E. Brun, *Helv. Phys. Acta* **43,** 799 (1970).
13. C. Prakash, *Hyperfine Interact.* **35,** 875 (1987).
14. A. Navrotsky, *Am. Mineral.* **71,** 1160 (1986).
15. J. C. Waerenborgh, Ph.D. dissertation. IST, Universidade Técnica de Lisboa, Lisboa, Portugal, 1992.
16. "International Tables for X-Ray Crystallography—Vol. 4: Revised and Supplementary Tables" (J. A. Ibers and W. C. Hamilton, eds.). Kynoch Press, Birmingham, England, 1974).
17. D. T. Cromer, *Acta Crystallogr.* **32,** 339 (1976).
18. D. T. Cromer and D. A. Liberman, *Acta Crystallogr.* **37,** 267 (1981).
19. D. B. Wiles and R. A. Young, *J. Appl. Crystallogr.* **14,** 149 (1981).
20. D. B. Wiles and R. A. Young, "User's Guide to DBW3.2s Program for Rietveld Analysis of X-Ray and Neutron Powder Diffraction Patterns (Version 8804)", p. 24, 1988).
21. J. Schneider, "IUCr International Workshop on the Rietveld Method." Petten, The Netherlands, 1989.
22. E. Hovestreydt, *Acta Crystallogr., Sect. A* **39,** 268 (1983).
23. G. Caglioti, A. Paoletti, and F. P. Ricci, *Nucl. Instrum.* **3,** 223 (1958).
24. A. J. Stone, appendix to G. M. Bancroft, A. G. Maddock, W. K. Ong, R. H. Prince, and A. J. Stone, *J. Chem. Soc. A,* 1966 (1967).
25. R. J. Hill, J. R. Craig, and G. V. Gibbs, *Phys. Chem. Miner.* **4,** 317 (1979).
26. R. D. Shannon, *Acta Crystallogr., Sect. A* **32,** 751 (1976).
27. H. St. C. O'Neill, W. A. Dollase, and C. R. Roth II, *Phys. Chem. Miner.* **18,** 302 (1991).
28. H. St. C. O'Neill, H. Annersten, and D. Virgo, *Am. Mineral.* **77,** 725 (1992).
29. J. N. Roelofsen, R. C. Peterson, and M. Raudsepp, *Am. Mineral.* **77,** 522 (1992).
30. P. Gütlich, R. Link, and A. Trautwein, "Mössbauer Spectroscopy and Transition Metal Chemistry." Springer-Verlag, Berlin, 1978.
31. E. Brunn, *Helv. Phys. Acta* **37,** 626 (1964).
32. B. J. Evans, S. S. Hafner, and H. P. Webber, *J. Chem. Phys.* **55,** 5282 (1971).
33. F. Menil, *J. Phys. Chem. Solids* **46**(7), 763 (1985).
34. Y. Zhang, *Inorg. Chem.* **21,** 3886 (1982).
35. A. Hudson and H. J. Whitfield, *Mol. Phys.* **12,** 165 (1967).
36. T. Mizoguchi and M. J. Tanaka, *J. Phys. Soc. Japan* **18,** 1301 (1963).
37. M. D. Osborne, M. E. Fleet, and G. M. Bancroft, *J. Solid State Chem.* **53,** 174 (1984).